CHEMISTRY OF MATERIALS
Article

Chem. Mater. **2010,** *22,* 1509–1520 1509
DOI:10.1021/cm903031d

Sol−Gel Processing of a Glycolated Cyclic Organosilane and Its Pyrolysis to Silicon Oxycarbide Monoliths with Multiscale Porosity and Large Surface Areas

Manuel Weinberger,[†,‡] Stephan Puchegger,[†] Thomas Fröschl,[‡] Florence Babonneau,[§] Herwig Peterlik,[†] and Nicola Hüsing*[,‡]

[†]Faculty of Physics, University of Vienna, Strudlhofgasse 4, A-1090 Vienna, Austria, [‡]Inorganic Chemistry I, Ulm University, Albert-Einstein Allee 11, D-89081 Ulm, Germany, and [§]Laboratoire de Chimie de la Matière Condensée de Paris, Université Pierre et Marie Curie, Collège de France and CNRS, UMR 7574, F-75005, Paris, France

Received September 30, 2009. Revised Manuscript Received December 2, 2009

This study is related to the preparation of silicon oxycarbide monoliths comprising a hierarchical network build-up from the pyrolysis of monolithic organosilica gels. A novel glycol-modified 1,3,5-trisilacyclohexane-carbosilane "$[Si(OCH_2CH_2OH)_2CH_2]_3$" was processed via a polymerization-induced phase separation process in hydrochloric acid solution containing the Pluronic P123 block copolymer and potassium chloride. Highly porous organosilica monoliths with interconnected macropores and a large amount of uniformly sized polymer-templated mesopores within the macroscopic framework domains were obtained after supercritical fluid extraction. The monoliths were pyrolyzed in argon atmosphere at 1000 °C to yield silicon oxycarbide monoliths by maintaining the hierarchical porosity of the organosilica gel. Both the organosilica gels and the silicon oxycarbide monoliths were thoroughly investigated with standard characterization techniques. If no salt was used for the preparation of organosilica gels, no distinct macroporous structures were obtained. Instead, the gels show the characteristics of typical aerogels with surface areas of 600−900 $m^2 g^{-1}$ and mesopores with pore sizes > 10 nm. A different behavior was observed if potassium chloride was added to the sols. Then, the system showed the tendency for a polymerization-induced phase separation leading to gels exhibiting multiscale porosity. The onset of the phase separation as well as the macropore/domain size thereby strongly depends on the concentration of KCl. These gels with a surface area of about 1070 $m^2 g^{-1}$ and pore diameters of about 11.6 nm were subjected to pyrolysis at 1000 °C under inert gas atmosphere. Although volume shrinkages of 54% were observed, the monoliths maintained their shape and structural features. The surface areas remained rather high with 531 $m^2 g^{-1}$, and the diameter of the mesopores dropped to 9.1 nm. From solid state NMR measurements and elemental analysis of the pyrolyzed sample, the formation of true silicon oxycarbide monoliths with multiscale porosity and a composition of $SiC_{0.23}O_{1.53} + 0.58C_{free}$ were proven. From resonant ultrasound spectroscopy measurements, a Young's modulus value of 1.42 GPa was obtained.

Introduction

Silicon oxycarbide (SiCO) materials offer several advantages compared to (organo) silica. The partial substitution of oxygen by carbidic carbon species inside an amorphous silicon dioxide phase improves the materials thermal,[1] chemical,[2] and mechanical properties.[3,4] Thus, these materials may be regarded as a modification of amorphous silica, which is suitable for application at extreme conditions. For example, the material overcomes the limited use of silica at high temperatures due to the high devitrification tendency, low viscosity together with high creep rates of the latter one. There are several routes for the preparation of SiCO materials. The most common approaches use the pyrolytic conversion of polyorganosiloxanes or polycarbosilanes at temperatures > 800 °C.[5−11] The molecular composition of the ceramic precursor has a direct influence on

---

*Corresponding author. E-mail: Nicola.huesing@uni-ulm.de.

(1) Rouxel, T.; Massouras, G.; Soraru, G.-D. *J. Sol-Gel Sci. Technol.* **1999**, *14*, 87.
(2) Soraru, G.-D.; Dallapiccola, E.; D'Andrea, G. *J. Am. Ceram. Soc.* **1996**, *79*, 2074.
(3) Soraru, G.-D.; Modena, S.; Guadagnino, E.; Colombo, P.; Egan, J.; Pantano, C. *J. Am. Ceram. Soc.* **2002**, *85*, 1529.
(4) Moysan, C.; Riedel, R.; Harshe, R.; Rouxel, T.; Augereau, F. *J. Eur. Ceram. Soc.* **2002**, *22*, 2389.
(5) Babonneau, F.; Thorne, K.; Mackenzie, J. D. *Chem. Mater.* **1989**, *1*, 554.
(6) Babonneau, F.; Bois, L.; Yang, C.-Y.; Interrante, L. V. *Chem. Mater.* **1994**, *6*, 51.
(7) Liu, Q.; Shi, W.; Babonneau, F.; Interrante, L. V. *Chem. Mater.* **1997**, *9*, 2434.
(8) Soraru, G. D.; Liu, Q.; Interrante, L. V.; Apple, T. *Chem. Mater.* **1998**, *10*, 4047.
(9) Corriu, R. J. P.; Leclercq, D.; Mutin, P. H.; Vioux, A. *J. Sol-Gel Sci. Technol.* **1997**, *8*, 327.
(10) Corriu, R. J. P.; Leclerq, D.; Mutin, P. H.; Vioux, A. *J. Mater. Sci.* **1995**, *30*, 2313.
(11) Kockrick, E.; Frind, R.; Rose, M.; Petasch, U.; Böhlmann, W.; Geiger, D.; Herrmann, M.; Kaskel, S. *J. Mater. Chem.* **2009**, *19*, 1543.

the final composition of the SiCO material. It was shown that the amount of carbidic carbon within the SiCO seems to be inversely related to the O/Si ratio of the preceramic species,[6,10] and it is also well-known that terminal alkyl groups, such as $\mathrm{Si{-}CH_3}$ give a poor carbidic carbon content.[6] It is thus reasonable to use a carbosilane with low oxygen content and mainly methylene groups, such as 1,1,3,3-tetraethoxy-1,3-disilacyclobutane, $\mathrm{[Si(OEt)_2CH_2]_2}$, or its ring-opening polymerization products.[7,8] Indeed, the carbidic carbon content in SiCO obtained from the pyrolysis of the polycondensation products of these precursors is rather high. However, the formation of an additional free carbon phase, which has only a minor influence on many properties of the SiCO and acts more or less as an inert secondary phase,[2] is a usual byproduct of the pyrolysis of organosilicas. Detailed studies have shown that carbon is formed during the pyrolysis at 500−600 °C via cracking and cyclization of aliphatic hydrocarbons.[12,13] The formation of this phase could be inhibited by incorporation of $\mathrm{Si{-}H}$ groups into the material. These groups will for example react with terminal methyl groups, which are in the initial material or formed in situ, to give $\mathrm{H_2}$ and a bridging methylene group.[14−16]

Due to the drastic pyrolysis conditions, it is still a challenging task to maintain the porosity of a SiCO precursor powder or gel. Only recently, some publications demonstrated the successful pyrolysis of mesostructured organosilica powders to SiCO ceramics by maintaining the mesoporous system and thus a large surface area.[17,18] Interestingly, whether or not a mesostructured SiCO is obtained seems to depend on the type of mesostructure itself. Detailed studies have shown that cubic mesostructures can be maintained very well, while the 2D hexagonally arranged mesopores will not lead to an SiCO but to phase-separated $\mathrm{SiO_2}$ and free carbon.[18−20] Until now, the reaction mechanism still remains unclear.

Most of SiCO materials are available only in form of powders or dense glasses. But for several applications, for example in catalysis, monoliths with multiscale porosity would be much more attractive. In recent years, great efforts were devoted to independently design structural features of materials on several length scales. This goal has already been achieved for silica and organosilica-based materials, for which monolithic materials (of several centimeters in size) comprising a macroporous network and disordered or even periodically ordered mesopores have successfully been prepared by utilizing phase separation phenomena of polymer mixtures, from which the macroscopic morphologies may be frozen by the concomitantly occurring sol−gel transition.[21−25,27−34] Inside the pore walls of the mesopores, one also may find micropores smaller than 2 nm. Such materials with multiscale porosity offer an excellent mass transfer through the material due to the macropores combined with large specific surface areas (from the mesopores) and therewith a lot of room for functionalization making these materials promising candidates for applications in chromatography or catalysis.

In 2003, two groups independently reported the preparation of silica monoliths with macropores and uniformly sized, periodically arranged mesopores within the framework domains. Hüsing et al. were applying tetrakis(2-hydroxyethoxy)silane in a sol−gel process containing the Pluronic P123 surfactant.[30] As was shown by SAXS studies,[26] the glycol released upon hydrolysis showed a better compatibility with surfactant mesophases from poly(alkylene oxide)-based surfactants than conventional alkoxides and therewith mesostructure formation and phase separation were facilitated. A unique, cellular macroscopic framework was obtained, with highly ordered 2D hexagonally arranged mesopores.[27] In another approach, Lindén et al. demonstrated the preparation of silica monoliths with multimodal hierarchical porosity via a double templating route using poly(ethylene oxide) as well as alkylammonium surfactants.[28] However, the templated mesopores showed a lower degree of periodicity than in P123 systems. A year later, Nakanishi et al. prepared the first organic−inorganic hybrid monoliths with a 2D hexagonal mesostructure from 1,2-bis(triethoxysilyl)ethane.[29] Since then various inorganic−organic hybrid materials[30−34] and even transition metal oxides with multiscale porosity have become accessible.[35,36]

The application of lyotropic phases as templates as well as the polymerization-induced phase separation process in the synthesis of multiscale materials rely to a large extent on a well-balanced polarity of the sol−gel system.

---

(12) Trassl, S.; Motz, G.; Rössler, E.; Ziegler, G. *J. Am. Ceram. Soc.* **2002**, *85*, 239.

(13) Trassl, S.; Kleebe, H.-J.; Störmer, H.; Motz, G.; Rössler, E.; Ziegler, G. *J. Am. Ceram. Soc.* **2002**, *85*, 1268.

(14) Babonneau, F.; Soraru, G. D.; D'Andrea, G.; Dirè, S.; Bois, L. *Mater. Res. Soc. Symp. Proc.* **1992**, *271*, 789.

(15) Sorarù, G. D.; D'Andrea, G.; Campostrini, R.; Babonneau, F.; Mariotto, G. *J. Am. Ceram. Soc.* **1995**, *78*, 379.

(16) Singh, A. K.; Pantano, C. G. *Mater. Res. Soc. Symp. Proc.* **1992**, *271*, 795.

(17) Pauletti, A.; Handjani, S.; Fernandez-Martin, C.; Gervais, C.; Babonneau, F. *J. Ceram. Soc. Jpn.* **2008**, *116*, 449.

(18) Toury, B.; Blum, R.; Goletto, V.; Babonneau, F. *J. Sol-Gel Sci. Technol.* **2005**, *33*, 99.

(19) Toury, B.; Babonneau, F. *J. Eur. Ceram. Soc.* **2005**, *25*, 265.

(20) Masse, S.; Laurent, G.; Babonneau, F. *J. Non-Cryst. Sol.* **2007**, *353*, 1109.

(21) Nakanishi, K.; Soga, N. *J. Am. Ceram. Soc.* **1991**, *74*, 2518.

(22) Nakanishi, K.; Komura, H.; Takahashi, R.; Soga, N *Bull. Chem. Soc. Jpn.* **1994**, *67*, 1327.

(23) Nakanishi, K. *J. Porous Mater.* **1997**, *4*, 67.

(24) Nakanishi, K.; Kanamori, K. *J. Mater. Chem.* **2005**, *15*, 3776.

(25) Nakanishi, K. *Bull. Chem. Soc. Jpn.* **2006**, *79*, 673.

(26) Ivanova, R.; Lindman, B.; Alexandridis, P. *Langmuir* **2000**, *16*, 3660.

(27) Hüsing, N.; Raab, C.; Torma, V.; Roig, A.; Peterlik, H. *Chem. Mater.* **2003**, *15*, 2690.

(28) Smått, J.-H.; Schunk, S.; Lindén, M. *Chem. Mater.* **2003**, *15*, 2354.

(29) Nakanishi, K.; Kobayashi, Y.; Amatani, T.; Hirao, K.; Kodaira, T. *Chem. Mater.* **2004**, *16*, 3652.

(30) Brandhuber, D.; Torma, V.; Raab, C.; Peterlik, H.; Kulak, A.; Hüsing, N. *Chem. Mater.* **2005**, *17*, 4262.

(31) Brandhuber, D.; Peterlik, H.; Hüsing, N. *Small* **2006**, *2*, 503.

(32) Hartmann, S.; Brandhuber, D.; Hüsing, N. *Acc. Chem. Res.* **2007**, *40*, 885.

(33) Nakanishi, K.; Amatani, T.; Yano, S.; Kodaira, T. *Chem. Mater.* **2008**, *20*, 1108.

(34) Weinberger, M.; Fröschl, T.; Puchegger, S.; Peterlik, H.; Hüsing, N. *Silicon* **2009**, *1*, 19.

(35) Konishi, J.; Fujita, K.; Nakanishi, K.; Hirao, K. *Chem. Mater.* **2006**, *18*, 864.

(36) Konishi, J.; Fujita, K.; Oiwa, S.; Nakanishi, K.; Hirao, K. *Chem. Mater.* **2008**, *20*, 2165.

With increasing complexity of e.g. bridged organosilanes, this balance is disturbed and the controlled formation of pores on several length scales becomes more difficult.

To our knowledge, few publications report the preparation of hierarchically structured ceramic materials. Smarsly and co-workers reported the successful preparation of hierarchically organized silicon carbide monoliths using the nanocasting approach with impregnation of hierarchically structured silica monoliths with mesophase pitch or furfuryl alcohol and subsequent carbothermal reduction.[37] Another interesting approach was presented by Schwieger et al.[38] They infiltrated Rattan with liquid silicon. The obtained silicon/silicon carbide composite was then coated with zeolites to finally generate a silicon/silicon carbide/zeolite composite ceramic with multiscale porosity.[38]

The present contribution demonstrates a new and original route for the preparation of hierarchically structured silicon oxycarbide monoliths and expands the availability of highly porous and thermally stable materials. We were able to prepare hierarchically structured organosilica monoliths from a modified 1,3,5-trisilacyclohexane carbosilane precursor. This precursor was chosen due to its low O/Si ratio and its potential as a sol−gel precursor for mesostructured materials.[39] The monoliths obtained from this precursor were subjected to pyrolysis at elevated temperature under inert gas atmosphere. The monolithic shape together with the structural features of the inorganic−organic hybrid monoliths in macroscopic and mesoscopic dimensions are still retained after the pyrolysis procedure. Solid-state magic angle spinning (MAS) NMR measurements, elemental analysis, and Raman spectroscopy prove the formation of a true silicon oxycarbide ceramic together with a free carbon phase. Additionally, the mechanical properties of the material were determined using resonant ultrasound spectroscopy.

Materials and Experimental

Chemicals. Chloromethyltrimethoxysilane was received from Wacker AG. Magnesium turnings (> 99%) were purchased from Merck, Pluronic P123 (M_n = 5800 g mol^{-1}) from Aldrich and potassium chloride (> 99.5%) from Fluka. These chemicals were used without further purification. Ethylene glycol (> 99.5%) was purchased from Merck and dried with sodium. The solvents tetrahydrofuran (THF) and pentane were distilled over sodium hydride dispersion.

Precursor Synthesis. All reactions were carried out with dried glassware in an argon atmosphere using the Schlenk technique.

Synthesis of 1,3,5-tris[dimethoxysila]cyclohexane [(MeO)$_2$SiCH$_2$]$_3$ (see the top part of Figure 1). A 45 g (1.85 mol) portion of magnesium turnings were given into 300 mL of THF. The solution was heated to 50 °C. To activate the magnesium, a spatula tip of iodine was added. The solution was stirred for 10 min, and then, a solution of 31.5 mL (0.21 mol) of chloromethyltrimethoxysilane in 300 mL of THF was added slowly via a dropping funnel. The mixture was kept at this temperature for 6 h and then cooled to room temperature and stirred overnight. The volatiles were removed by distillation and the residues were extracted with 200 mL of pentane and filtered. The pentane was then evaporated to yield 14.49 g of a colorless liquid consisting of a mixture of several silanes.[40] Via distillation 5.01 g (16 mmol) of the desired product were obtained (65−67 °C at 0.1 mbar) in 23% yield.

^{1}H NMR (400.13 MHz, d_6-benzene, δ): 0.19 (s, 6H, $-$Si$-$C$H_2$$-Si-$), 3.40 (s, 18H, $-$Si$-$O$-$CH_3). ^{13}C NMR (100.62 MHz, d_6-benzene, δ): $-$1.68 ($-$Si$-$$CH_2$$-Si-$), 50.23 ($-Si-O-$$CH_3$); ^{29}Si NMR (79.49 MHz, d_6-benzene, δ): $-$4.91 ([(MeO$_2$)SiCH$_2$]$_3$).

Transesterification with Ethylene Glycol. A 5.01 g (16 mmol) portion of 1,3,5-tris(dimethoxysila)cyclohexane was mixed with 16.1 mL (0.29 mol) of ethylene glycol. The mixture was heated to 140 °C under vigorous stirring. Most of the methanol was removed via distillation. Subsequently, the remaining methanol and an excess of ethylene glycol were removed by vacuum distillation yielding almost quantitatively 7.76 g of a glassy solid (theoretical yield for complete conversion: 7.88 g). The silicon content of the precursor was determined by thermogravimetric analysis to be 16.96%. This is in accordance with the theoretically expected value for a 1:2 ratio of silicon to glycol of 17.1%.

Preparation of Organosilica Monoliths. Pluronic P123 was mixed with 0.1 M aqueous hydrochloric acid solution in mass fractions of 10:90, 15:85, 20:80, and 30:70. In a typical gel synthesis, 0.3 g of potassium chloride was added to 3.26 g of a 20:80 polymer solution (1.5 mol L^{-1} KCl referred to the amount of HCl solution). A 1 g portion of the glassy precursor was pulverized and given to the solution at ambient conditions under vigorous stirring. The amount of silicon in grams with respect to the amount of Pluronic P123 and HCl solution in grams gives a ratio of 5.2/20/80 g. This results in the identifier 5.2:20:80, if the gel was prepared in the absence of KCl. If the HCl solution is 1.5 M in KCl, the identifier changes to 5.2:20:80@1.5 M. The sols were kept in sealed cylindrical sample tubes for gelation and aging at 40 °C. Opaqueness indicating phase separation occurred within the first hour followed by gelation several minutes thereafter. Gels which were prepared without salt showed no phase separation prior to gelation. For the 5.2:20:80@1.5 M composition, wet gels were washed two times with 0.1 M aqueous hydrochloric acid and three times with ethanol within 48 h to remove most of the salt and polymer. The other samples, whether they were prepared with different amounts of salt or without salt, were washed five times with ethanol within 48 h. All gels were dried via supercritical solvent extraction with CO$_2$ to yield opaque and crack-free monoliths (in the abscence of salt or after washing with hydrochloric acid solution). Cracks occurred during extraction of Pluronic P123, if ethanol was used as extraction solvent, probably due to osmotic pressure or crystallization of KCl.

Pyrolysis of Organosilica Monoliths. The 5.2:20:80@1.5 M monoliths were put inside a corundum tube which was placed in a tubular furnace. In a flow of argon (50 mL min^{-1}), the samples were heated within 2.5 h to 120 °C and kept there for 0.5 h. Within 3 h, the system was heated to 1000 °C. The temperature was kept there for another 2 h, followed by cooling under argon flow to room temperature. The resulting materials can be described as crack-free and dark brown to black colored monoliths. The ceramic yield is about 83%.

---

(37) Sonnenburg, K.; Adelhelm, P.; Antonietti, M.; Smarsly, B.; Nöske, R.; Strauch, P. *Phys. Chem. Chem. Phys.* **2006**, *8*, 3561.

(38) Zampieri, A.; Kullmann, S.; Selvam, T.; Bauer, J.; Schwieger, W.; Sieber, H.; Fey, T.; Greil, P. *Microporous Mesoporous Mater.* **2006**, *90*, 162.

(39) Landskron, K.; Hatton, B. D.; Perovic, D. D.; Ozin, G. A. *Science* **2003**, *302*, 266.

(40) Brondani, D. J.; Corriu, R. J. P.; El Ayoubi, S.; Moreau, J. J. E.; Wong Chi Man, M. *Tetrahedron Lett.* **1993**, *34*, 2111.

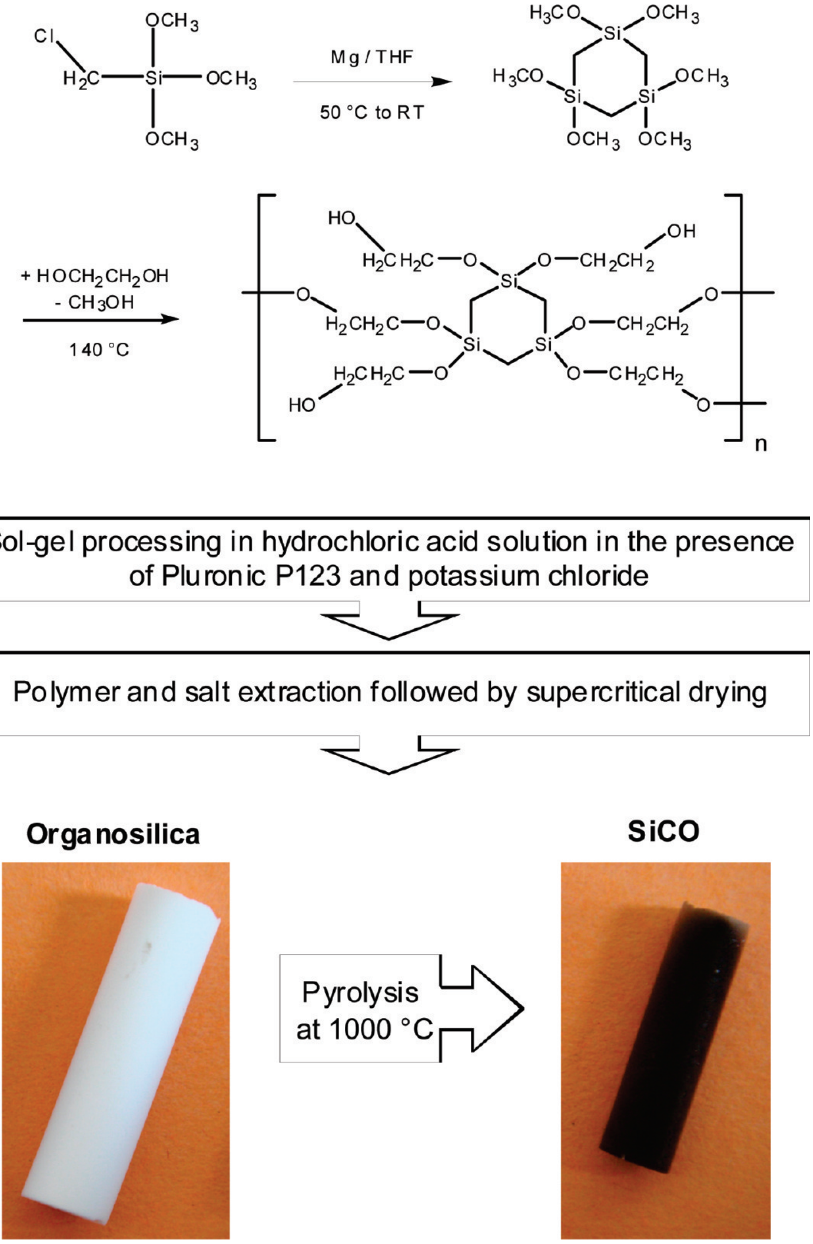

Figure 1. Preparation scheme of silicon oxycarbide monoliths (diameter of the organosilica monolith ca. 5 mm).

Characterization. Nuclear magnetic resonance (NMR) spectra of the precursor were acquired on a Bruker Avance DRX 400. Dried deuterated d_6-benzene was used as solvent.

The solid state NMR spectroscopy was performed on a Bruker AVANCE 500 spectrometer (11.75 T), except the ^{29}Si single pulse MAS spectrum on the organosilica sample, which was recorded on a Bruker AVANCE 300 spectrometer (7.05 T). Here, 7 mm double resonance MAS probe heads were used with 5 kHz spinning rate. Long recycle delays were used for the ^{29}Si single pulse MAS spectra to account for long T_1 relaxation times, and allow for quantitative analysis of the spectra (100 s and 45° pulse for the organosilica sample and 150 s and 90° pulse for the SiCO sample). Contact times of 3 and 1 ms were used for ^{29}Si and ^{13}C CP-MAS spectra, respectively. Simulations of the spectra were obtained using the dmfit software.[41]

Small angle X-ray scattering measurements of the dried organosilica as well as of the pyrolyzed samples were performed in vacuum using a rotating anode X-ray generator (Nanostar, Bruker AXS) with an X-ray beam monochromatized and collimated from crossed Goebel mirrors. The scattering was collected with a 2D position sensitive detector (Vantec 2000). The samples were prepared as powders and pasted between two Scotch tapes. The resulting SAXS patterns were radially averaged to obtain the intensity in dependence of the scattering vector $q = (4\pi/\lambda)\sin(\theta)$. 2θ is the scattering angle and $\lambda = 0.1542$ nm is the X-ray wavelength. Measurements were carried out at two different distances (11 and 107 cm) to cover a wide q range from 0.07 to 15 nm^{-1}.

The morphology of the materials was investigated by scanning electron microscopy (SEM) with a Zeiss DSM 692 operating at 15 kV (for low resolution images) and with a Zeiss Supra 55 VP operating at 5 kV (for high resolution images) on gel pieces sputtered with AuPd. The lower nanometer regime was investigated by transmission electron microscopy (TEM) using a Philips 400T operating at 80 kV.

---

(41) Massiot, D.; Fayon, F.; Capron, M.; King, I.; Le Calvé, S.; Alonso, B.; Durand, J.-O.; Bujoll, B.; Gan, Z.; Hoatson, G. *Magn. Reson. Chem.* **2002**, *40*, 70.

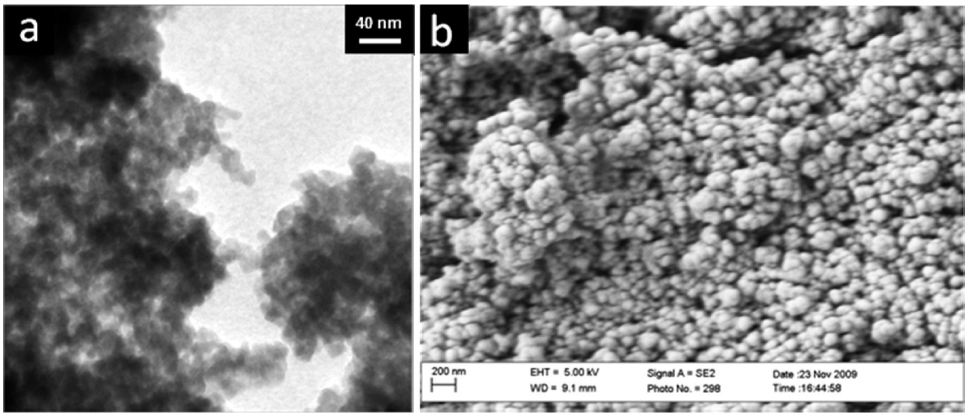

Figure 2. Electron microscopy images of the sample 5.2:20:80: (a) TEM; (b) SEM.

Nitrogen sorption measurements were performed at 77 K on a Quadrasorb SI (Quantachrome). The samples were outgassed in vacuum at 100 °C prior to the measurement. The specific surface areas were determined by application of the Brunauer/Emmett/Teller (BET) equation in the lower relative pressure range ($p/p_0 = 0.05-0.15$), where the isotherm behaves in a linear fashion. The pore size distributions were obtained by Barrett/Joyner/Halenda (BJH) analysis of the adsorption branch of the isotherm.

Thermogravimetric measurements of the precursor and the organosilica material were performed on a Netzsch STA 449 C Jupiter. In both cases, a heating rate of 10 K min^{-1} was used. Raman spectra were recorded on a Labram spectrometer from Horiba Jobin Yvon GmbH with a laser wavelength of 632.82 nm. Elemental analysis was performed on a 2400 CHN Elemental Analyzer from Perkin-Elmer. The elastic moduli were determined using a self-developed dynamical measuring equipment based on resonance vibrations (Elastotron 2000) and complete numerical data evaluation (resonant ultrasound spectroscopy). The evaluation method RUS is based on the numerical determination of the resonance frequencies of freely vibrating bodies, which can be solved for simple shapes such as cylinders, rods and spheres.[42]

Results and Discussion

Highly porous silicon oxycarbide monoliths with multiscale porosity were obtained from pyrolysis of organosilica monoliths which were prepared via sol–gel processing of a glycol-modified trisilacyclohexane-carbosilane in aqueous hydrochloric acid solution in the presence of the Pluronic P123 surfactant and potassium chloride (Figure 1).

Preparation of the Organosilica Gels. The successful preparation of hierarchically organized silsesquioxane monoliths from a glycol-modified bis-silylated ethane has been shown by our group in previous work.[34] Such hierarchically structured materials were obtained for a wide range of synthesis parameters. The morphology of the gel skeleton and the size of the macroscopic framework domains comprising periodically arranged mesopores can be influenced by the P123/acid ratio. In contrast to these results, increasing the size of the organosilane precursor from a simple ethane-bridged derivative to a dendrimeric structure (4,4,10,10-tetraethoxy-7,7-bis[2-(triethoxysilyl)ethyl]-3,11-dioxa-4,7,10-trisilatridecane) always resulted in highly porous materials consisting of 3-dimensionally connected particles with average diameters of about 10–20 nm[43] exhibiting no hierarchical build-up of the network. In that case, no macroscopic phase separation was observed for the applied wide variation of the synthesis parameters indicating a pronounced difference in the polarity of the mixture, and thus a disturbed tendency for phase separation in addition to a different hydrolysis and condensation kinetics. If one considers the increased surface density of condensable groups of the dendrimer (12 compared to 6), a fast branching of the units could lead to a kinetically frozen state.

First sol–gel experiments with the glycol-modified 1,3,5-tris[dimethoxysila]cyclohexane indicated a chemical behavior similar to that of the dendrimer. We varied the mass fractions of Pluronic P123 to 0.1 M aqueous hydrochloric acid solution from 10/90 up to 30/70 by keeping the precursor concentration constant. Within this region, macroscopic phase separation is easily observed for the glycol-modified bis-silylated ethane precursor. But for the cyclic derivative, only translucent wet gels were formed indicating the absence of larger framework domains.

Investigations of the macroscopic morphology by electron microscopy were performed on different gels prepared using a fixed amount of precursor and a variation of the P123/0.1 M hydrochloric acid ratio. No significant influence of the sol composition on the final gel structure is observed. Figure 2 shows TEM and SEM images for the 5.2:20:80 gel, which are representative images for all these gels. In the nanometer regime, the system consists of 3-dimensionally interconnected particles with a size of about 10 nm (Figure 2a). As expected from the translucent appearance of the gels, there is no significant macroscopic porosity seen in the SEM images (Figure 2b). Similar gels were obtained even in the absence of the surfactant (gel 4.9:0:80) indicating a sol–gel behavior similar to the one seen for the carbosilane dendrimer resulting in nanoporous gels.

---

(42) Migliori, A.; Sarrao, J. L. *Resonant Ultrasound Spectroscopy*; John Wiley & Sons, Inc.: New York, 1997.

(43) Weinberger, M.; Puchegger, S.; Rentenberger, C.; Puchberger, M.; Hüsing, N.; Peterlik, H. *J. Mater. Chem.* **2008**, *18*, 4783.

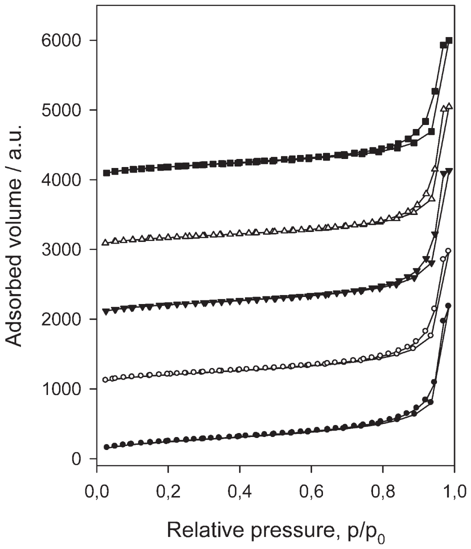

Figure 3. Sorption measurements for nanoporous aerogels: (filled circles) 4.9:0:80; (open circles) 5.2:10:90; (filled triangles) 5.2:15:85; (open triangles) 5.2:20:80; (filled squares) 5.2:30:70.

Table 1. Structural Parameters for the Nanoporous Aerogels Derived from the Cyclic Glycolated Silane

	nitrogen sorption		SAXS	
sample	S^{BET}/m^2 g^{-1}	V^{ta}/cm^{3}g^{-1}	D	ξ/nm
4.9:0:80	868	3.37	2.76	10
5.2:10:90	738	3.04	2.74	7.8
5.2:15:85	750	3.3	2.8	7.06
5.2:20:80	626	3.16	2.82	6.65
5.2:30:70	676	3.09	2.84	6.27

[a] Total pore volumes were estimated from the last point of the adsorption isotherms.

From nitrogen sorption measurements (see Figure 3), typical type IV isotherms were obtained with a very late and steep increase of the adsorbed volume indicating large mesopores. BJH analysis of the desorption branch confirms the presence of pores of about 10 nm in diameter with a broad size distribution typical for silica aerogels. A significant microporosity was not observed, and the specific surface areas are in the range of 600−900 m^2 g^{-1}. The exact values are given in Table 1.

SAXS has proven to be an excellent tool to analyze the nanostructure of such gels in detail. In Figure 4, the SAXS patterns for various gels obtained from the cyclic silane in the presence of different surfactant concentrations are shown. The formation of a periodic mesostructure with a long-range order was not observed; however, a short-range order peak at about 10 nm^{-1} is visible. This peak can be assigned to molecular building blocks with a diameter d in real space of approximately 0.6 nm. Toward low q-values, the curves display the typical scattering of silica aerogels.[43]

To gain structural information, the SAXS intensities were fitted with a model based on spherical molecular building blocks with the specific diameter obtained from the short-range order peak and building up a network with correlation length ξ and a fractal dimension D as previously successfully used to describe the scattering for gels derived from the carbosilane dendrimer. The correlation length is directly related to the cluster size,[44] which is also qualitatively accessible from TEM images. The results are given in Table 1. The fractal dimension of about $D = 2.8$, and the correlation length of about 10 nm lead to the conclusion that the molecular building blocks build up a three-dimensional network, which is relatively dense on the cluster scale of ten to some tenth of nanometers. As seen in Table 1, there is a trend that the size of the clusters decrease with an increasing P123/hydrochloric acid ratio, similar to the case of dendrimer-derived organosilicas. A possible explanation is that the polymer blocks the free silanol groups and therewith suppresses further condensation reactions, from which a larger particle size is obtained.

As can be seen from the above results, it was not possible to induce macroscopic phase separation under the given synthesis parameters by simply processing the glycolated cyclic silane in surfactant/water solutions. This might be due to the change in polarity, but also due to the change in the sol−gel reaction kinetics compared to other glycolated silanes such as the ethylene-bridged derivative or tetrakis(2-hydroxyethyl)orthosilicate. It is known from literature that inorganic salts have a strong influence on phase separation phenomena.[28,45,46] The colloidal particles or hybrid micelles formed during the precursor polymerization will be stabilized due to the positive surface charge given under acidic conditions; however, agglomeration of these species is then hindered. Thus larger aggregates may not be obtained, and the tendency for phase separation is decreased. Addition of a salt, such as potassium chloride, will increase the ionic strength, and therefore, the surface charge may be better shielded. By this, the potential barrier between the colloidal species is decreased and agglomeration is facilitated. In addition, the agglomeration of more hydrophobic organosilica oligomers with surfactant micelles should also be facilitated due to the dehydration of the poly(ethylene oxide) moieties of the outer shell of the micelles by the Cl$^-$ anions.[47] If these assumptions are correct, it should be possible to control the phase separation and with it the macroscopic morphology of the final gel network as well as the formation of mesostructures by addition of different amounts of potassium chloride (0 up to 2 M aqueous solutions) to the 5.2:20:80 sol. A first promising indication of a phase separation was observed as all gels turned opaque prior to gelation. The onset of the change in transparency of the gel depends strongly on the concentration of KCl with larger amounts resulting in faster change. Up to a concentration of 1.5 M aqueous KCl, homogeneous wet gels are formed; a concentration of 2 M will lead to precipitation, most probably due to the formation of very large aggregates. After gelation and aging, the gels were washed with ethanol and finally dried

---

(44) Teixeira, J. *J. Appl. Crystallogr.* **1988**, *21*, 781.
(45) Zhong, H.; Liu, J.; Wang, P.; Yang, J.; Yang, Q. *Microporous Mesoporous Mater.* **2009**, *123*, 63.
(46) Yu, C.; Fan, J.; Tian, B.; Zhao, D. *Chem. Mater.* **2004**, *16*, 889.
(47) Guo, W.; Park, J.-Y.; Oh, M.-O.; Jeong, H.-W.; Cho, W.-J.; Kim, I.; Ha, C.-S. *Chem. Mater.* **2003**, *15*, 2295.

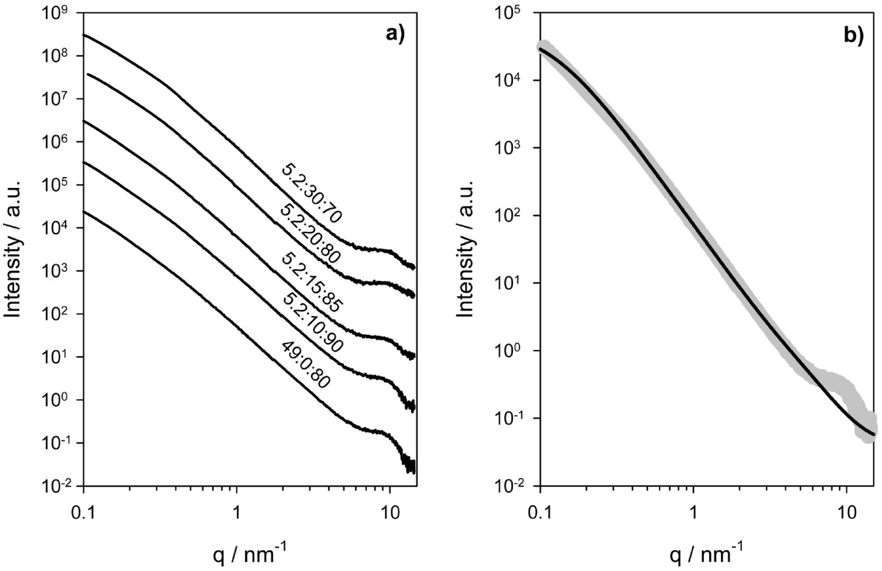

Figure 4. (a) SAXS measurements of the organosilica aerogels. (b) Exemplary fit of the 5.2:10:90 gel.

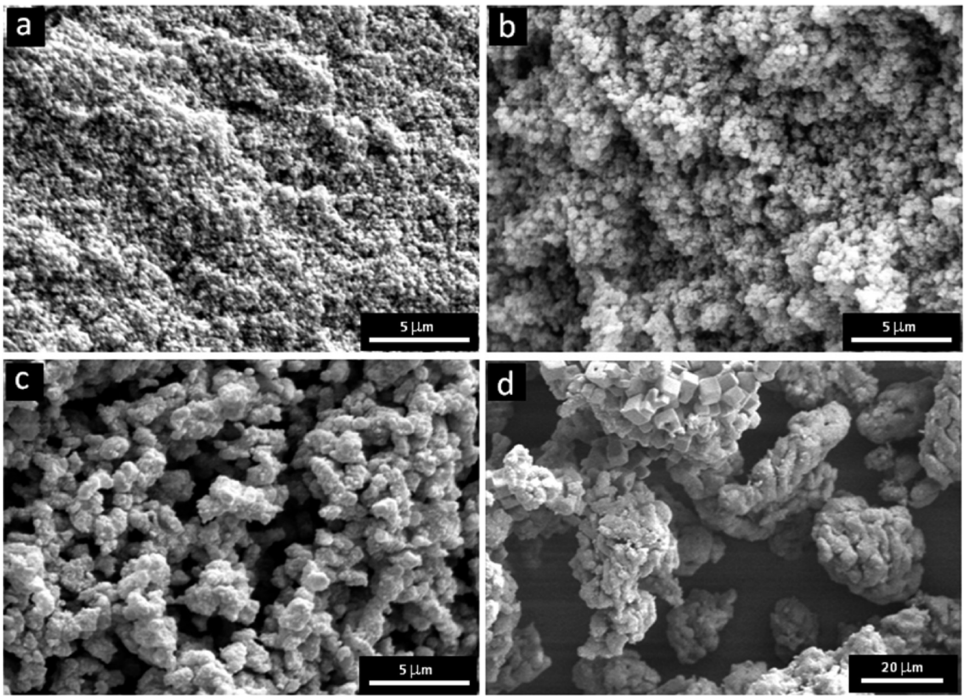

Figure 5. SEM images for gels which were prepared with different amounts of salt (a) 0, (b) 1.25, (c) 1.5, and (d) 2 M. Note the different scale bar of 20 μm, and the cubic KCl crystals for (d) after washing with ethanol.

supercritically. The powder was also washed with ethanol, but dried at ambient conditions.

Since KCl is not soluble in ethanol, an osmotic pressure or the crystallization of KCl will lead to a cracking of the monoliths. Washing with water or hydrochloric acid solution allows the maintenance of the monolithic shape. In Figure 5, SEM images of the macroscopic frameworks are shown. The increase of the domain size with increasing amount of salt is clearly seen. From 0 up to 1.25 M, the differences are rather small (about 250 nm), but with larger amounts of KCl the size of the particles increases drastically to about 900 nm. This can be explained by a coarsening during the intermediate stage of the spinodal decomposition.[23] The sooner the phase separation occurs compared to the gelation of the system, the larger the domains may grow. For 1.5 M, we obtained a gel showing the cocontinuous characteristics of a spinodally phase separated system. Remaining KCl crystals are clearly visible in Figure 5d; however, all samples still contain a significant amount of the salt.

Figure 6a shows a sample washed with hydrochloric acid prior to the drying process, thus allowing for a direct comparison with the gels from washing with ethanol (Figure 5c). The gels display a similar framework domain size, but the gel washed with ethanol shows a coarser structure probably due to remaining KCl. In the following we will concentrate the discussion for the pyrolyzed samples on the structural

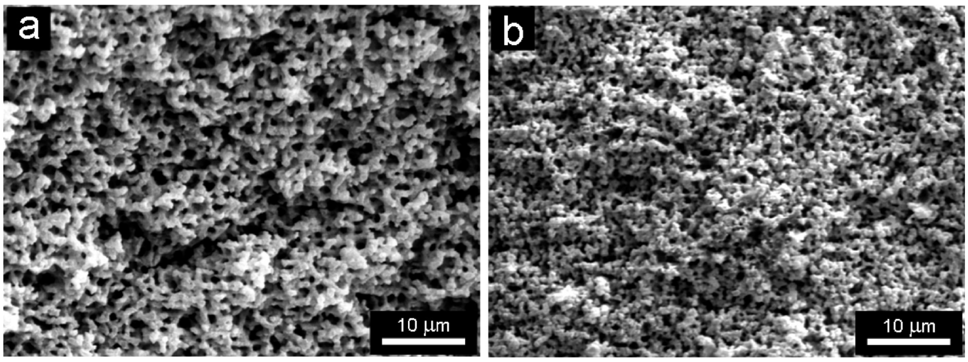

Figure 6. Comparison of SEM images for (a) organosilica 5.2:20:80@1.5 M and (b) the corresponding silicon oxycarbide.

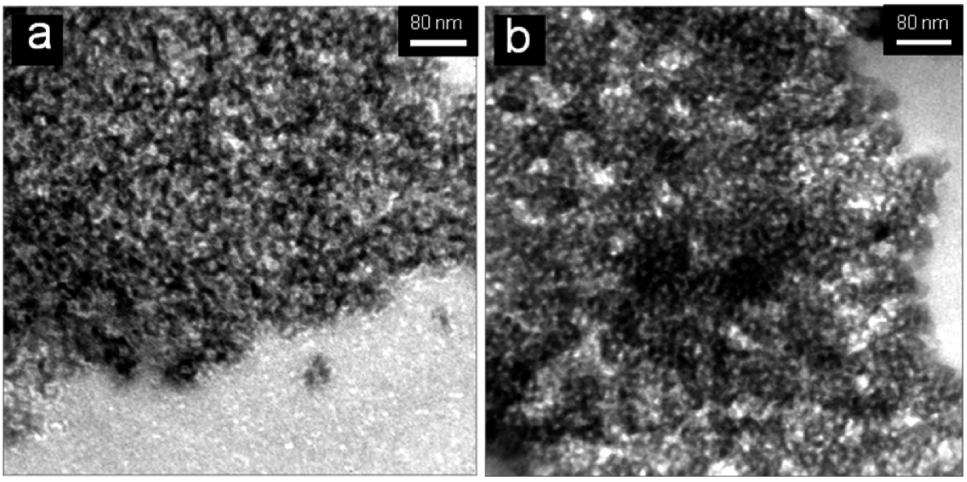

Figure 7. Comparison of TEM images for (a) organosilica 5.2:20:80@1.5 M and (b) corresponding silicon oxycarbide.

and chemical characterization of gels prepared with 1.5 M KCl and subsequently washed with aqueous hydrochloric acid, since here KCl was removed completely as was shown by XRD and XPS measurements of the pyrolyzed samples.

With similar sol−gel processing conditions we have previously demonstrated that the surfactant Pluronic P123 is not only able to induce a macroscopic phase separation but also acts as a structure directing agent to give highly ordered mesostructures. Template removal then gives access to the corresponding mesopores. It was shown that the mesostructure formation is directly connected to the phase separation, and the mechanism of this process may be understood as a nucleation of hybrid micelles and the growth of the nucleation sites by consumption of other hybrid micelles for example to 2D hexagonally arranged mesopores.[34] In the case of the glycolated cyclic silane, TEM investigations of the salt effect on the mesostructure have shown that no distinct periodic mesostructures are obtained for salt concentrations lower than 1 M, but for larger salt concentrations, we observed the formation of weakly ordered MSU-like mesostructures.[48] In the TEM images, micelle templated mesopores are clearly seen (Figure 7a).

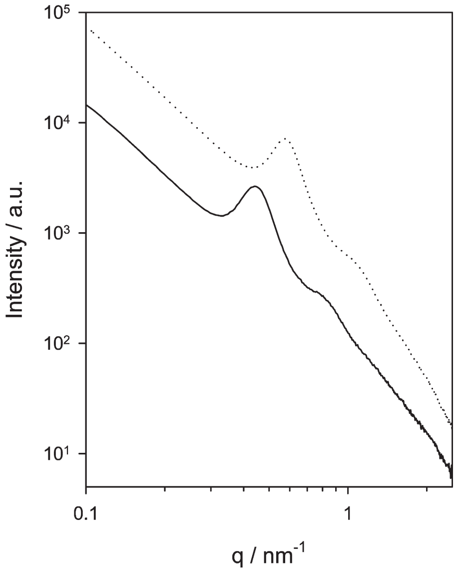

Figure 8. SAXS measurements for the organosilica 5.2:20:80@1.5 M (continuous line) and SiCO (dotted line) material.

SAXS measurements (continuous line in Figure 8) show an intense but broad peak at low $q = 0.44$ nm^{-1} (corresponding d-spacing $d_{\max} = 14.3$ nm) and a shoulder at larger $q = 0.6$ nm^{-1} (corresponding d-spacing = 10.5 nm). Such scattering patterns are usually obtained for wormholelike mesostructures,[49] thus confirming the results

---

(48) Bagshaw, S. A.; Prouzet, E.; Pinnavaia, T. J. *Science* **1995**, *269*, 1242.

(49) Prouzet, E.; Cot, F.; Nabias, G.; Larbot, A.; Kooyman, P.; Pinnavaia, T. J. *Chem. Mater.* **1999**, *11*, 1498.

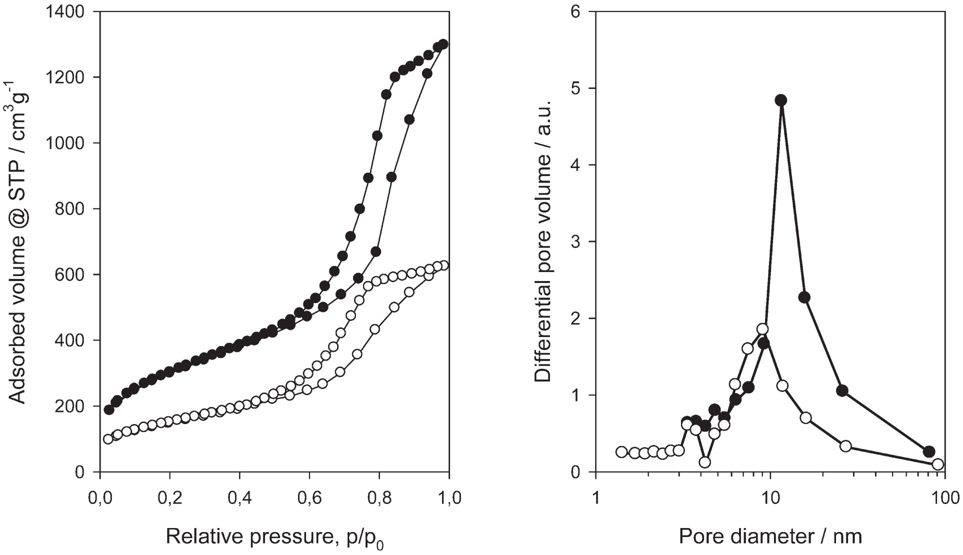

Figure 9. Comparison of nitrogen sorption data: sorption isotherms (left) and pore size distributions (right); (filled circles) organosilica, (open circles) SiCO.

from electron microscopy. Although the hybrid micelles give weakly ordered nanostructures, we assume a mechanism for the mesostructure formation that is induced by a preceding phase separation leading to a metastable state and thus favoring nucleation and growth routes. A reason for the absence of nanostructures with a mesoscopic ordering in the case of the gels prepared with lower salt concentrations could be the late onset of the macroscopic phase separation. Thereby the sol−gel transition may proceed, leading to highly branched species showing a lower flexibility and thus no tendency for nucleation and growth.

Nitrogen sorption measurements for the organosilica gel show type IV isotherms with a H2 type hysteresis loop typical for periodic mesoporous materials (see the curve with filled circles in Figure 9 on the left). The BET surface area is rather large $S^{BET} = 1070$ m^2 g^{-1}. Moreover, desorption seems not to be greatly delayed indicating an open mesoporous system. The material exhibits an extraordinarily large total pore volume of 2 cm^3 g^{-1}. Compared to the gels obtained from the glycol-modified ethane-bridged silane system[34] with pore diameters of 4.8−5.5 nm, the mesopores are very large (maximum in pore size distribution: $d^{BJH} = 11.6$ nm) as is seen from the late and steep increase of the adsorption branch (capillary condensation) and the corresponding BJH analysis (see curve with filled circles in Figure 9 on the right). The salt seems to have a significant influence on the pore size. The chloride anions could lead to a dehydration of the outer shell of the micelles, thus the hydrophilicity of the poly(ethylene oxide) moieties is decreased and the outer shell is less accessible to species such as the oligomeric silane precursor molecules. This could probably lead to a thinner hydrophilic shell and therefore to an enlarged hydrophobic core and thus larger mesopores. Regarding the phase separation, another explanation is that the newly formed phase rich in hybrid micelles could favor larger micelle radii due its polarity. However, more detailed studies in the future have to be applied for a better understanding of this pore expanding phenomenon.

To get information on the chemical composition of the materials solid state ^{29}Si and ^{13}C MAS NMR measurements were performed (Figure 10). Interrante and coworkers published an investigation of the polycondensation products of the 1,3-bis[dimethoxysila]cyclobutane carbosilane by NMR measurements.[7] The silane was condensed at ambient conditions and then either vacuum-dried at 50 °C or dried at ambient pressure at 160 °C. The vacuum-dried product showed a D-unit peak as expected for the four membered ring, but the other material contained a significant amount of cleaved Si−C bonds leading to the formation of T-units. Although the six-membered ring should show a minimum of ring tension, it is of interest if such phenomena are also observable in the present case since the precursor was transalkoxylated at around 140 °C. In Figure 10b, the ^{29}Si NMR spectrum of the polymer, salt extracted, and dried organosilica material is shown. There are three peaks at −8.15 (weak shoulder), −17.04, and −23.60 ppm, which can be assigned to the D-units D_0 $(CH_2)_2Si(OH)_2$, D_1 $(CH_2)_2Si(OSi)(OH)$, and D_2 $(CH_2)_2$-$Si(OSi)_2$ with the following relative intensities of 7%, 48%, and 45%, respectively.[39] In the ^{13}C NMR spectrum in Figure 10a, we observed a peak at 7.40 ppm which is characteristic for bridging methylene groups.[39] However, two peaks at 16.3 and 57.8 ppm indicate the presence of ethoxy groups, probably formed during the washing procedure with ethanol and some smaller signals can be assigned to residual P123 block copolymer (70.74 ppm; $-OCH_2$-CH_2O-), to the methyl groups of residual methoxy groups (47.49 ppm) and most probably to residual glycol groups (63.42 ppm). Both measurements indicate that the molecular structure of the precursor is maintained upon transesterification with ethylene glycol and the subsequent acid-catalyzed condensation reaction.

We could show that it is possible to prepare hierarchically organized inorganic−organic hybrid monoliths

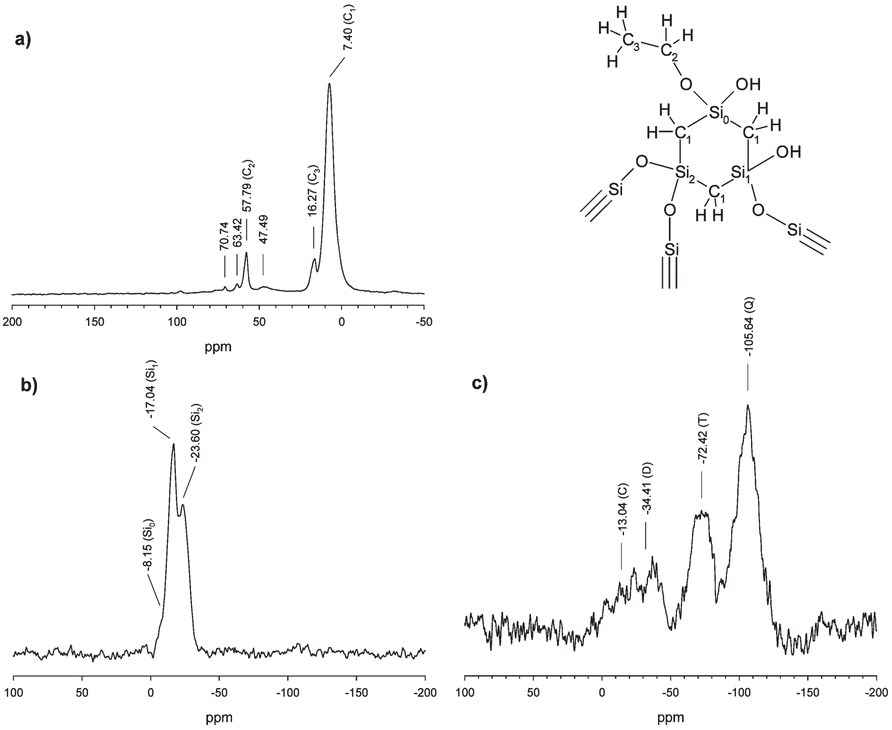

Figure 10. (a) ^{13}C NMR spectra of organosilica and comparison of ^{29}Si NMR spectra for (b) organosilica and (c) corresponding silicon oxycarbide.

comprising a macrocellular network and uniform mesopores from a glycolated cyclic silane by the addition of salt to the silane/water/surfactant precursor mixture. Such cocontinuous network structures combined with a large mesopore volume and high specific surface areas are desirable for many applications. To improve the thermal and mechanical strength of these hybrid materials, the monoliths obtained from 1.5 M KCl solution were pyrolyzed to yield silicon oxycarbide ceramic materials.

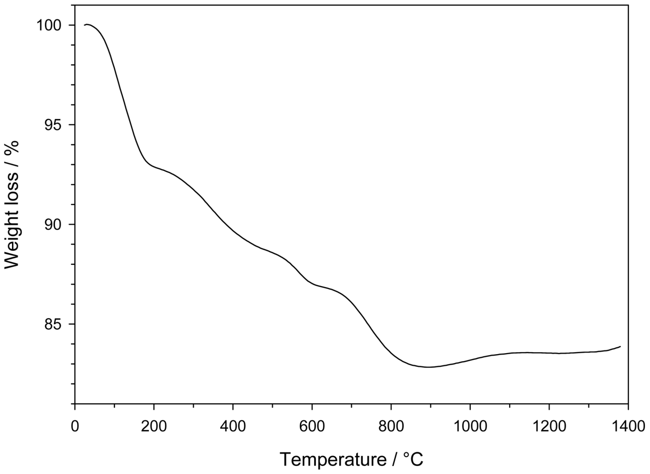

Figure 11. Thermogravimetric measurement of the pyrolysis of the organosilica.

Pyrolysis of Organosilicas. The thermal treatment of the porous organosilica monoliths was investigated in detail via thermogravimetric analysis from room temperature up to 1400 °C in nitrogen atmosphere (Figure 11). The curve progression agrees well with literature results (see for instance refs 6 and 7). In the temperature range from RT up to 200 °C, a weight loss of about 7.2% is observed, which can be assigned to the desorption of water. The following weight losses up to 600 °C of about 5.9% occur most probably due to the thermal decomposition of remaining P123, further condensation reactions releasing water and ethanol and minor decomposition reactions of the framework. The rearrangement of the Si$-$O and Si$-$C bonds starts at temperatures higher than 600 °C with a final weight loss of 4%. The sum of the weight losses is 17.2%, resulting in a ceramic yield of 82,8%, which is in good agreement with the ceramic yield of the pyrolyzed monoliths. However, one has to be careful with the interpretation of the TG results. At higher temperatures, the sample gains about 1% of weight. This can, on the one hand, be attributed to an artifact, which is probably caused by the experimental setup or, on the other hand, to minor oxidation due to invasion by air. Although, the slope of the curve agrees well with literature results, the occurrence of oxygen would lead to a larger extent of decomposition than is the case in a totally inert atmosphere. The residue of the thermally treated material was black probably due to the formation of a free carbon phase. Wide angle XRD measurement showed no SiC peaks indicating that no carbothermal reduction occurred.

Due to the stability of the material at temperatures above 1000 °C as seen from thermogravimetric measurements, the material should also withstand a longer thermal treatment of 2 h. This is necessary for a complete conversion of the organosilica monoliths into SiCO and for a further stabilization of the network. Indeed, the monolithic shape could be maintained (see Figure 1), but an average volume-shrinkage of about 54% is observed.

Table 2. Structural Parameters for the 5.2:20:80@1.5 M Gel and the SiCO

	nitrogen sorption		SAXS	
sample	S^{BET}/ m^2 g^{-1}	V^{t}[a]/ cm^3 g^{-1}	D^{BJH}/nm	d_{max}/nm
5.2:20:80@1.5 M	1071	2	11.6	14.3
SiCO	531	0.97	9.1	11

[a] Total pore volumes were estimated from the last point of the adsorption isotherms.

However, from a structural point of view, a quite unique behavior is observed with a very homogeneous shrinkage of the whole network. SEM and TEM images in Figures 6b and 7b show that the domain sizes as well as the macropores shrink by approximately 50%, but the filigree interconnected pore structure is maintained. The bicontinuous framework obviously has the capability to withstand the stress occurring during the decomposition and reorganization of the molecular moieties of the organosilica material. In addition, the mesostructure within the macroscopic framework domains has shrunk, but is maintained, as can be clearly seen in the TEM images as well as in the SAXS investigations (see dotted line in Figure 8). The *d*-spacing for the intense peak at low q is shifted to larger $q = 0.57$ nm^{-1} (corresponding *d*-spacing = 11 nm). From sorption measurements (see curve with open circles in Figure 6 on the left), we observe a drop of the surface area from 1070 m^2 g^{-1} for the initial organosilica to 530 m^2 g^{-1} for the SiCO what would still be rather high if a true silicon oxycarbide was obtained. There is still a huge mesopore volume present (approximately 50%) that is seen from capillary condensation at large relative pressures, and the corresponding total pore volume was estimated to be 0.97 cm^3 g^{-1}. The hysteresis indicates that the mesopore system is still very accessible. From BJH analysis, it is seen that the maximum in the pore diameter distribution is shifted to smaller values (from 11.6 to 9.1 nm). The comparison of the structural parameters of the 5.2:20:80@1.5 M gel and the pyrolyzed sample is given in Table 2.

A silicon oxycarbide is a silicon dioxide matrix in which divalent oxygen is partly substituted by tetravalent carbidic carbon. ^{29}Si MAS NMR measurements are the most straightforward method to deduce if a true silicon oxycarbide material was formed and to describe the composition of the material quantitatively. In the ^{29}Si MAS NMR spectrum, we should see a distribution of $\mathrm{SiC}_x\mathrm{O}_{4-x}$ units with $x = 0$ (Q-units), $x = 1$ (T-units), $x = 2$ (D-units), $x = 3$ (M-units) and $x = 4$ (C-units). And indeed, the pyrolysis procedure applied is leading to a rearrangement and redistribution of the carbon and silicon species, and we observe several peaks in the NMR spectrum (Figure 10 c), which can be attributed to the above-mentioned species. In our case, we obtained four peaks at −105.64 (Q-units, 48.3%), −72.42 (T-units, 29%), −34.41 (D-units, 13.4%) and −13.04 (C-units, 9.3%). Since the formation of the SiCO is accompanied by the formation of a free carbon phase, as indicated by the occurrence of Q-units in the ^{29}Si NMR spectrum and the black color of the monoliths, quantitative information of the amount of this free carbon phase is necessary in order to give a complete quantitative description. With Raman spectroscopy, the formation of the free carbon phase could be evidenced by the occurrence of two bands: one at 1334.1 cm^{-1} characteristic for disordered carbons such as glassy carbon and one band at 1597.2 cm^{-1} which is probably observed due to the occurrence of tiny graphene layers with many edge carbons.[50] C/H/N elemental analysis was performed to estimate the whole amount of carbon within the pyrolyzed sample. Therefore it was possible to estimate the following formula, $\mathrm{SiC}_{0.23}\mathrm{O}_{1.53} + 0.58\mathrm{C}_{\mathrm{free}}$ from which we may conclude the formation of a material rather rich in carbidic carbon if we compare our results to the mesostructured SiCOs of Pauletti et al. ($\mathrm{SiC}_{0.17}\mathrm{O}_{1.66} + 0.45\mathrm{C}_{\mathrm{free}}$)[17] or Toury et al. ($\mathrm{SiC}_{0.11}\mathrm{O}_{1.78} + 0.66\mathrm{C}_{\mathrm{free}}$).[18]

The elastic properties of the hierarchically organized SiCO cylinders were determined in a dynamical resonance system. The cylindrical sample is clamped carefully between two piezoelectric transducers: one to excite the sample and the other to detect the answer (i.e., the resonance frequencies). Both transducers are connected to a network analyzer, which is able to sweep a wide frequency range with an extremely high signal-to-noise ratio. Nevertheless, the damping of the organosilica monoliths was so high that no resonance frequencies could be determined, whereas from the SiCO cylinder, clear resonances were obtained. The material with a density of about 0.4 g cm^{-3} has a Young's modulus of 1.42 GPa and a shear modulus of 0.54 GPa. This is significantly higher than the value of silica monoliths (70 MPa) with a similar hierarchical structure and a density of 0.21 g cm^{-3} or the value of 100 MPa of silica aerogels with a comparable density.[51] Though the density of the SiCO is slightly higher, the Young's modulus exceeds the one of comparable silica materials by more than 1 order of magnitude. This is attributed to the higher binding energy of SiC bonds in comparison to silica bonds and is of the same size than the ratio of dense SiC ceramics in relation to dense silica glasses. More detailed studies of the influence of processing parameters and the amount of incorporated carbidic carbon on the elastic properties will be the subject of future research.

There are only a few publications which investigate and discuss the possibility of the pyrolytic conversion of mesostructured organosilicas into the corresponding silicon oxycarbides by maintaining the mesostructural features. Toury et al. and Pauletti et al. have demonstrated the successful SiCO preparation from ethylene-bridged and mesostructured silsesquioxanes obtained from sol−gel processing of the corresponding bis-silylated alkoxysilane.[17,18] However, the amount of carbidic carbon within these powder materials is low compared to many other SiCO materials. There is also a restriction to cubic mesostructures since it seems not possible to obtain SiCO from 2D hexagonally arranged cylindrical

---

(50) Fukushima, M.; Yasuda, E.; Teranishi, Y.; Nakamura, K.; Tanabe, Y. *J. Ceram. Soc. Jpn.* **2004**, *112*, 612.

(51) Puchegger, S.; Brandhuber, D.; Hüsing, N.; Peterlik, H. *J. Non-Cryst. Solids* **2006**, *352*, 5251.

mesopores. The approach presented here to prepare (organo)silica monoliths with multiscale porosity from a cyclic carbosilane with bridging methylene groups and thus to reduce the O/Si ratio, resulting in a material richer in carbidic carbon, was a quite challenging task. However, the preparation of the desired material was successfully achieved and the pyrolytic conversion gave a material much richer in carbidic carbon and even the structural features could be maintained at all length scales. Thus, a first step toward the preparation of a new class of monolithic materials with multiscale porosity and improved thermal and mechanical properties is made.

Conclusions

The carbosilane 1,3,5-tris[dimethoxysila]cyclohexane was synthesized by a Grignard reaction of chloromethyltrimethoxysilane. The obtained cyclic precursor was successfully modified with ethylene glycol without Si−C-bond cleavage to yield a highly water-soluble sol−gel precursor. Organosilica gels were prepared via sol−gel processing in hydrochloric acid solution in the presence of the block copolymer Pluronic P123. After polymer extraction and supercritical drying, highly porous organosilica monoliths were obtained. Within a wide range of synthesis parameters, no distinct phase separation phenomena and mesostructure formation were observed. However, upon addition of potassium chloride, macroscopic phase separation was successfully induced. Depending on the amount of KCl, the onset of the phase separation and the morphology of the macroscopic framework domains could be deliberately controlled. If the concentration of KCl was chosen to be 1.5 M, a cocontinuous framework structure was achieved with a huge amount of wormholelike mesopores within the framework domains, and thus, this material shows a huge surface area of 1071 $m^2\ g^{-1}$. Both ^{13}C and ^{29}Si MAS solid state NMR measurements showed that the gel truly consists of the polycondensed cyclic precursor species and no Si−C-bond cleavage occurred during precursor and gel synthesis.

This organosilica material was subsequently pyrolyzed at 1000 °C under an inert gas atmosphere. The appearance changed from white to black, and volume shrinkages of 54% were observed; however, the monolithic shape could be maintained. Detailed electron microscopy investigations revealed that the framework and macropores as well as the mesopores shrunk homogeneously. The surface area decreased to 531 $m^2\ g^{-1}$. From Raman spectroscopy, the formation of a free carbon phase was observed. To elucidate if a true silicon oxycarbide material was formed, quantitative ^{29}Si MAS solid state NMR measurements were performed. The best fit of the spectra with Gaussian functions gave four peaks which can be assigned to a distribution of Q-, T-, D- and C-units of a silicon oxycarbide. Together with the determination of the whole carbon content by elemental analysis, the following formula can be estimated to be $SiC_{0.23}O_{1.53} + 0.58C_{free}$. First resonant ultrasound spectroscopy measurements revealed a Young's modulus of 1.42 GPa which is significantly higher than that of similar silica systems.

Acknowledgment. M.W. is grateful for financial support from the Initiative College "Experimental Materials Science−Nanostructured Materials" of the University of Vienna. The support from FWF project 20767-N20 is acknowledged. We are indebted to Prof. Bogdan Sepiol and Prof. Michael Wong Chi Man for helpful discussions.